Theoretical assessment on the validity of the Wiedemann-Franz law for icosahedral quasicrystals

Enrique Maciá* and Rogelio Rodríguez-Oliveros
Departamento de Física de Materiales, Facultad de Ciencias Físicas, Universidad Complutense de Madrid, E-28040 Madrid, Spain
(Received 23 January 2007; published 29 March 2007)

The validity of the Wiedemann-Franz law (WFL) for icosahedral quasicrystals belonging to the families AlCu(Fe,Ru) and AlPd(Mn,Re) is discussed. We exploit some characteristic features in the electronic structure in order to obtain closed analytical expressions for the transport coefficients in terms of the Hurwitz zeta function. Depending on the Fermi-level position, a systematic deviation from the ideal WFL is observed. The role of self-similar features in the electronic structure on the WFL is discussed. The obtained expression for the Lorenz function may be used in order to refine previous experimental results on the charge-carrier contribution to the thermal conductivity in these materials.

DOI: 10.1103/PhysRevB.75.104210 PACS number(s): 61.44.Br, 71.23.Ft, 72.15.−v, 72.15.Cz

I. INTRODUCTION

The Wiedemann-Franz law (WFL) links the electrical conductivity, $\sigma(T)$, and the charge-carrier contribution to the thermal conductivity, $\kappa_e(T)$, of a substance by means of the relationship $\kappa_e(T)/\sigma(T)=L_0T$, where T is the temperature and $L_0=(k_B/e)^2\eta_0$ is the Lorenz number, where k_B is the Boltzmann constant, e is the electron charge, and η_0 depends on the sample's nature. Thus, for metallic systems $\eta_0=\pi^2/3$, and we get the Sommerfeld value $L_0=2.44\times10^{-8}\ \mathrm{V^2\,K^{-2}}$, while for semiconductors we have $\eta_0\simeq2$.[1] The WFL expresses a transport symmetry arising from the fact that the motion of the carriers determines both the electrical and thermal currents at low temperatures. As the temperature of the sample is progressively increased, the validity of WFL will depend on the nature of the interaction between the charge carriers and the different scattering sources present in the solid. In general, the WFL applies as long as elastic processes dominate the transport coefficients, and usually holds for arbitrary band structures provided that the change in energy due to collisions is small compared with k_BT.[2,3] Accordingly, one expects some appreciable deviation from WFL when electron-phonon interactions, affecting in a dissimilar way electrical and heat currents, start to play a significant role.[4] On the other hand, at high enough temperatures the heat transfer is dominated by the charge carriers again due to umklapp phonon-scattering processes, and the WFL is expected to hold as well.

Quasicrystals (QCs) are metallic alloys belonging to the class of aperiodic crystals. Since QCs consist of metallic elements, one should expect they would behave as metals do, hence reasonably obeying the WFL. This working hypothesis is routinely assumed when studying the thermal transport properties of these materials in order to estimate the phonon contribution to the thermal conductivity, $\kappa_{ph}(T)$, by subtracting from the experimental data, $\kappa_{mes}(T)$, the expected electronic contribution according to the expression $\kappa_{ph}=\kappa_{mes}-L_0T\sigma$. Nonetheless, it is now well established that most transport properties of stable QCs are quite unusual by the standard of common metallic alloys, resembling more semiconductorlike than metallic character.[5–9] Accordingly, it seems quite convenient to check the validity of this law for QCs, since our understanding of thermal properties in these materials should be substantially revised if it does not hold.[10]

To this end, we shall consider the following realistic model for the spectral conductivity close to the Fermi level:[11–14]

$$\sigma(E)=\bar{\sigma}\left\{\frac{\gamma_1}{(E-\delta_1)^2+\gamma_1^2}+\frac{\alpha\gamma_2}{(E-\delta_2)^2+\gamma_2^2}\right\}^{-1}, \qquad (1)$$

which satisfactorily describes the electronic structure of both QCs and approximant phases belonging to the AlCu(Fe,Ru) and AlPd(Mn,Re) icosahedral families in terms of a wide Lorentzian peak (related to the Hume-Rothery mechanism) plus a narrow Lorentzian peak (related to *sp-d* hybridization effects). This model includes six parameters, determining the Lorentzian heights ($\bar{\sigma}/\gamma_i$) and widths ($\sim\gamma_i$), their positions with respect to the Fermi level, δ_i, and their relative weight in the overall structure, $\alpha>0$. The parameter $\bar{\sigma}$ is a scale factor measured in $(\Omega\,\mathrm{cm\,eV})^{-1}$ units. Suitable values for these electronic model parameters can be obtained by properly combining *ab initio* calculations of approximant phases with experimental transport data of icosahedral samples within a phenomenological approach.[11,12,15–18]

II. ANALYTICAL EXPRESSIONS

Following previous works, we will express the Lorenz function in the form[18,19]

$$L(T)\equiv\frac{\kappa_e(T)}{T\sigma(T)}=\left(\frac{k_B}{eJ_0}\right)^2\begin{vmatrix}J_0 & J_1\\ J_1 & J_2\end{vmatrix}, \qquad (2)$$

where the kinetic coefficients J_i can be written as

$$J_0c_0^{-1}=\frac{4\pi^2}{3}\beta^{-2}+a_3\beta^{-1}H_1+a_4H_0+4a_0,$$

$$J_1c_0^{-1}=\frac{4\pi^2}{3}a_1\beta^{-1}+a_5H_1+a_3\beta G_0,$$

$$J_2c_0^{-1}=\frac{28\pi^4}{15}\beta^{-2}+a_6\beta H_1+a_5G_0\beta^2+\frac{4\pi^2}{3}a_0, \qquad (3)$$

where $c_0\equiv\bar{\sigma}(\gamma_1+\alpha\gamma_2)^{-1}$ and $\beta\equiv(k_BT)^{-1}$; the coefficients a_i were defined in Ref. 19, and we have introduced the auxiliary integrals

 ©2007 The American Physical Society

$$H_k(\beta) \equiv \int_{-\infty}^{\infty} \frac{x^k}{\beta^{-2}x^2 - 2\beta^{-1}q_1 x + q_0} \operatorname{sech}^2(x/2)dx, \quad (4)$$

and $G_0 \equiv 4 - q_0 H_0$, where $x \equiv \beta(E-\mu)$, E is the electron energy, $q_0 \equiv \varepsilon\varepsilon_1^2\varepsilon_2^2(\gamma_1+\alpha\gamma_2)^{-1}$, $q_1 = (\gamma_1\delta_2 + \alpha\delta_1\gamma_2)(\gamma_1+\alpha\gamma_2)^{-1}$, $\varepsilon_i^2 \equiv \gamma_i^2 + \delta_i^2$, and $\varepsilon \equiv \gamma_1\varepsilon_1^{-2} + \alpha\gamma_2\varepsilon_2^{-2}$. In order to evaluate these integrals, in previous works we expanded Eq. (4) in Taylor series around the Fermi level, concluding that QCs closely obey the WFL over a wide temperature range.[18] Subsequently, we realized that truncation effects have an important influence on the obtained results, so that the Lorenz function significantly deviates from its ideal behavior above ~50 K.[19]

Following a phenomenological approach, which allows one to extract suitable information about the electronic structure from the temperature dependence of the transport coefficient curves, the values $q_1 = -0.025$ eV, $q_1 = -0.015$ eV, and $q_1 = -8.8 \times 10^{-5}$ eV were respectively obtained for AlMnSi approximant phases,[17] *i*-AlCuFe QCs,[16] and *i*-AlPdRe QCs.[20] We notice that the smaller q_1 values correspond to high quality QCs, exhibiting long-range quasiperiodic order, whereas the larger value is obtained for an approximant crystal. Accordingly, we can confidently assume that the limiting behavior $q_1 \to 0$ properly applies to ideal QCs. The condition $q_1 = 0$ imposes the constraint

$$\frac{\delta_2}{\delta_1} = -\alpha\frac{\gamma_2}{\gamma_1} \quad (5)$$

among the model parameters. From a physical viewpoint, this relation indicates that (i) the peak location ratio is proportional to their height ratio, providing a characteristic correlation in the electronic structure, and (ii) since $\gamma_i > 0$, the Fermi level must be located in between both spectral features.

By inspecting Eq. (4), we realize that the auxiliary integral H_1 identically vanishes in the case $q_1 = 0$ due to the odd parity of the integrand. In that case, one obtains the closed analytical expression $H_0 = 4q_0^{-1}\tilde{\beta}\zeta_H(2, 1/2 + \tilde{\beta})$ (see the Appendix), where $\tilde{\beta} \equiv \sqrt{q_0}\beta/2\pi$ is a scaled variable and $\zeta_H(s,a) \equiv \Sigma_{k=0}^{\infty}(k+a)^{-s}$ is the Hurwitz zeta function, which reduces to the Riemann zeta function in the case $a = 1$.[21] By making use of this analytic expression, along with $H_1 = 0$, Eq. (3) can be rearranged in the matrix form

$$\begin{pmatrix} J_0 \\ J_1 \\ J_2 \end{pmatrix} = \frac{4\pi^2 c_0}{3} \begin{pmatrix} \frac{3}{\pi^2}\tilde{J}_{00} & 0 & 1 \\ 0 & \tilde{J}_{11} & 0 \\ \tilde{J}_{20} & 0 & \frac{7\pi^2}{5} \end{pmatrix} \begin{pmatrix} 1 \\ \beta^{-1} \\ \beta^{-2} \end{pmatrix}, \quad (6)$$

where $\tilde{J}_{00} \equiv a_0 + a_4 q_0^{-1}\tilde{\beta}\zeta_H$, $\tilde{J}_{11} \equiv a_1 + 12a_3 q_0^{-1} f(\tilde{\beta})$, and $\tilde{J}_{20} \equiv a_0 + 12a_4 q_0^{-1} f(\tilde{\beta})$, with $f(\tilde{\beta}) \equiv \tilde{\beta}^2(1 - \tilde{\beta}\zeta_H)$. By comparing Eq. (6) with Eq. (A12) in Ref. 19, and taking into account the asymptotic limits

$$\lim_{\tilde{\beta}\to\infty} \tilde{\beta}\varsigma_H = 1, \quad \lim_{\tilde{\beta}\to\infty} \tilde{\beta}^2(1 - \tilde{\beta}\varsigma_H) = 1/12, \quad (7)$$

we realize that the $\tilde{J}_{ij}(\tilde{\beta})$ coefficients reduce to $J_{ij}(q_1 = 0)$, so that the exact and approximate (Taylor expanded) expressions for the kinetic coefficients J_i coincide in the low-temperature regime. As the temperature is increased, however, the analytical expression given by Eq. (6) retains all the temperature dependent information contained in the kinetic coefficients in terms of the Hurwitz zeta function. Plugging the kinetic coefficient expressions given by Eq. (6) into Eq. (2), we obtain

$$L(T) = L_0 \frac{\tilde{J}_{00}\tilde{J}_{20} + Q(\tilde{\beta})\beta^{-2} + \frac{7\pi^4}{15}\beta^{-4}}{\tilde{J}_{00}^2 + \frac{2\pi^2}{3}\tilde{J}_{00}\beta^{-2} + \frac{\pi^4}{9}\beta^{-4}}, \quad (8)$$

where $Q(\tilde{\beta}) \equiv \pi^2(21\tilde{J}_{00}/5 + \tilde{J}_{20} - \tilde{J}_{11}^2)/3$. Making use of Eq. (7), one gets $\lim_{T\to 0} L(T) = L_0$, so that the WFL holds in the low-temperature regime, as expected. On the other hand, making use of the limits

$$\lim_{\tilde{\beta}\to 0} \tilde{\beta}\varsigma_H = 0, \quad \lim_{\tilde{\beta}\to 0} \tilde{\beta}^2(1 - \tilde{\beta}\varsigma_H) = 0 \quad (9)$$

in Eq. (8), one obtains the high-temperature limit $\lim_{T\to\infty} L(T) = 21L_0/5$. Therefore, we conclude that the WFL is obeyed by those QCs whose electronic structure close to the Fermi level can be properly described in terms of the spectral function given by Eq. (1) in both the low- and high-temperature regimes, although in the latter case the Lorenz number is 4.2 times larger than the Sommerfeld value.[22]

III. DISCUSSION

In order to illustrate the temperature variation of the Lorenz function, we evaluate Eq. (8) by making use of the electronic structure model parameters listed in Table I to obtain the curves shown in Fig. 1. The referenced values are taken from *ab initio* calculations for three representative QC samples. The remaining values have been derived from the *ab initio* ones by properly imposing the constraint $q_1 = 0$. Two main criteria have been adopted to this end: (i) to vary the relative position of the Fermi level (describing possible stoichiometric effects) or (ii) to vary the narrow spectral feature γ_2 parameter (describing both temperature and long-range resonance effects). By inspecting Fig. 1, the following conclusions can be drawn. First, the WFL is closely followed by most considered samples in the low-temperature regime. Second, significant deviations from the WFL are exhibited by those systems for which the condition $q_1 = 0$ is accomplished by tuning the Fermi-level relative position (dashed-line curves). In particular, by inspecting Table I, we clearly appreciate that the $L(T)$ curve deviation intensifies as E_F approaches the narrow spectral peak, irrespective of the sample nature.

On the other hand, in Fig. 1(d) we illustrate the high-temperature asymptotic limit prescribed by Eq. (8) for all the

TABLE I. Values of the electronic model parameters adopted to determine the Lorenz curves plotted in Fig. 1 (more details in the text).

Sample	γ_1	γ_2	δ_1	δ_2	α	q_1	$\frac{L[300]}{L_0}$
AlCuFe[a]	1.35	0.04	−0.12	0.23	0.98	0.220	
AlCuFe-1	1.35	2.64	−0.12	0.23	0.98	0	1.002
AlCuFe-2	1.35	0.04	−0.325	0.01	1	0	2.310
AlCuRu[12]	1	0.045	−1.1	0.275	1.7	0.177	
AlCuRu-3	1	0.125	−1.1	0.275	2	0	0.967
AlCuRu-4	1	0.045	−1.5	0.115	1.7	0	0.949
AlPdRe[b]	1.35	0.042	−0.2	0.23	3.864	0.184	
AlPdRe-5	1.35	0.388	−0.2	0.23	4	0	1.005
AlPdRe-6	1.35	0.042	−0.6	0.072	3.864	0	1.058

[a]Reference 11.
[b]Reference 12.

considered samples. As we can see, the theoretical limit $21L_0/5$ is attained at very high temperatures, well above the melting point of these materials (~1000 K). A suitable experimental measure of the WFL's validity over a given temperature range can be gained from the study of the magnitude $\kappa_{mes}(T)/\sigma(T)=L(T)+\varphi(T)$, where $\varphi(T)$ accounts for the phonon contribution to the heat transport. A study of the temperature variation of the κ_{mes}/σ ratio in several intermetallic compounds showed that the experimental data may be fitted by a linear temperature dependence of the form $\kappa_{mes}/\sigma=LT+B$ over the temperature range 350–800 K.[23,24] By comparing the slopes obtained for pure aluminum and icosahedral AlCuFe samples, the ratio $L_{QC}/L_{Al}\simeq 1.21$ was obtained, hence indicating an enhanced Lorenz number for QCs at high temperatures. In a similar way, room-temperature $L(T)$ values larger than L_0 have been experimentally reported, ranging from $L_{300}/L_0=1.15$ (Ref. 25) to $L_{300}/L_0=1.43$.[26] Therefore, the available experimental information supports the theoretical trend $L(T)/L_0>1$, prescribed by Eq. (8) in the high-temperature regime.

In order to gain some understanding of the observed deviation from the WFL in the intermediate temperature range, we will explicitly consider the thermal and electrical conductivities, which can be obtained from the expressions[18,19]

$$\kappa_e(T)=\left(\frac{k_B}{2e}\right)^2\left(J_2-\frac{J_1^2}{J_0}\right)T, \quad \sigma(T)=\frac{J_0}{4}. \tag{10}$$

Making use of Eq. (6), we can write Eq. (10) in the form

$$\kappa_e(T)=c_0L_0T\left(\frac{7\pi^2}{5}\beta^{-2}+\tilde{J}_{20}-\tilde{J}_{11}^2+\frac{\tilde{J}_{11}^2}{1+\frac{\pi^2}{3}\tilde{J}_{00}^{-1}\beta^{-2}}\right), \tag{11}$$

$$\sigma(T)=c_0\left(\frac{\pi^2}{3}\beta^{-2}+\tilde{J}_{00}\right). \tag{12}$$

By assuming that the limits given by Eq. (7) still hold in the considered temperature range, and keeping the leading terms in β^{-2} in Eqs. (11) and (12), we obtain the following approximate expression for the reduced Lorenz function:

$$\frac{L(T)}{L_0}=\frac{1+\frac{21}{5}\eta bT^2}{1+\eta bT^2}, \tag{13}$$

where $b\equiv e^2L_0=2.44\ \mathrm{eV}^2\ \mathrm{K}^{-2}$, and the coefficient

$$\eta\equiv\frac{\varepsilon_1^2\varepsilon_2^2(\delta_1-\delta_2)}{\delta_1\varepsilon_2^2-\delta_2\varepsilon_1^2} \quad (\text{in } \mathrm{eV}^{-2}) \tag{14}$$

accounts for electronic structure effects on the transport properties at the intermediate temperature range. Since $\varepsilon_i^2\neq 0$, Eqs. (13) and (14) indicate that the deviation from the WFL naturally occurs for any electronic structure (except for the trivial case $\delta_2=\delta_1$). The question regarding what sort of electronic structures will minimize and/or maximize the role of coefficient η in Eq. (13) then arises. To discuss this issue, we will first consider the temperature variation of the Lorenz function for actual samples. In Fig. 2, we show the normalized $L(T)$ curves, obtained from Eq. (8), for two representative samples of the icosahedral AlCuFe family, with $q_1=0$ eV and $\eta=0.055\ \mathrm{eV}^{-2}$ (solid line) and $q_1=0.015$ eV and $\eta=0.0022\ \mathrm{eV}^{-2}$ (dashed line), along with the approximant phase AlMnSi with $q_1=-0.025$ eV and $\eta=0.0019\ \mathrm{eV}^{-2}$ (dot-dashed line). The electronic model parameters adopted for the samples with $q_1\neq 0$ have been obtained from the analysis of experimental transport curves, as previously reported in Refs. 17 and 16 for AlMnSi and AlCuFe, respectively. By inspecting this figure, we observe a clear correlation between the nature of the long-range order present in the sample (roughly measured in terms of the q_1 parameter) and an enhancement of the $L(T)$ curve as compared to that prescribed by the WFL (horizontal solid line). In fact, whereas the approximant phase (exhibiting long-range periodic order) closely obeys the WFL over a broad temperature range (from 0 up to ~100 K),[27] the icosahedral AlCuFe samples (characterized by a long-range quasiperiodic order instead) exhibit an anomalous enhancement starting at low temperatures (~20 K). Such enhancement is also observed for the approx-

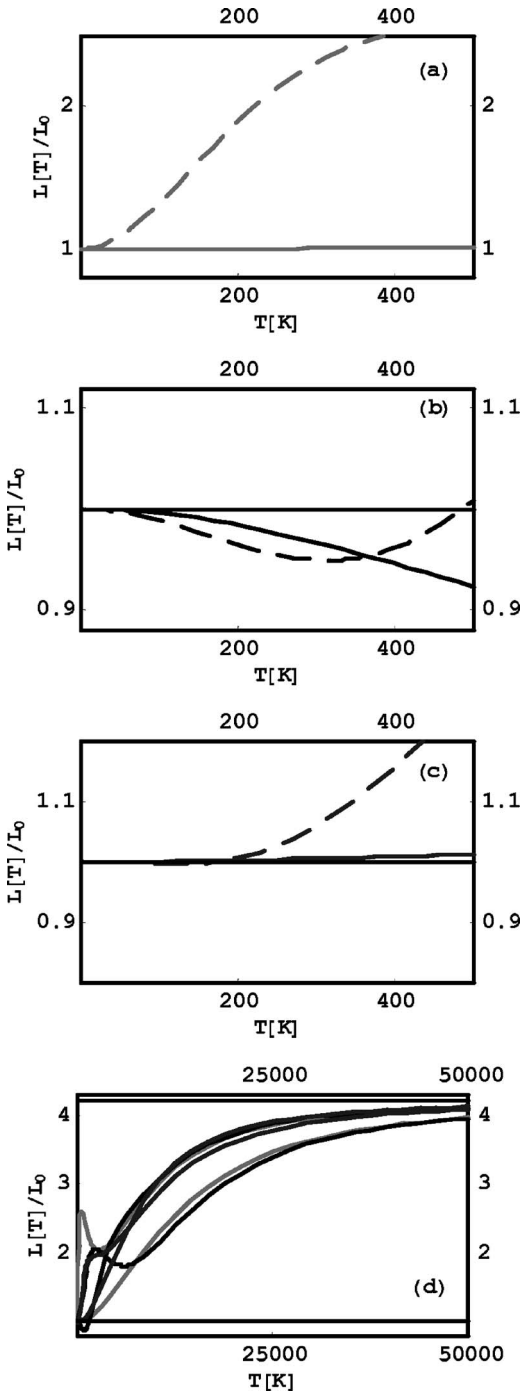

FIG. 1. Temperature variation of the normalized Lorenz function for (a) *i*-AlCuFe phases with the model parameters set respectively labeled 1 (solid line) and 2 (dashed line) in Table I, (b) AlCuRu phases with the model parameters set respectively labeled 3 (solid line) and 4 (dashed line) in Table I, and (c) AlPdRe phases with the model parameters set respectively labeled 5 (solid line) and 6 (dashed line) in Table I. In (d), we illustrate the high-temperature asymptotic limit for samples 1–6.

imant phase, but only at significantly higher temperatures. It is then tempting to assume that the observed enhancement in the $L(T)/L_0$ ratio may be related to the possible presence of self-similar features in the electronic structure of QCs. In order to check this point, we shall consider a representative

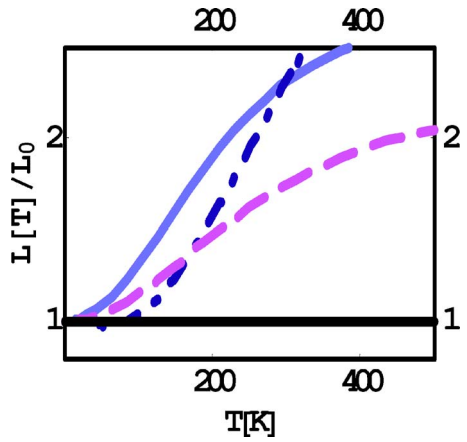

FIG. 2. (Color online) Temperature variation of the normalized Lorenz function for two samples of the icosahedral quasicrystal AlCuFe, with $q_1=0$ eV (solid line) and $q_1=0.015$ eV (dashed line), along with the approximant phase AlMnSi with $q_1=-0.025$ eV (dot-dashed line).

self-similar spectral conductivity model given by the parameters $\delta_1 \equiv -\tau^3\delta$, $\delta_2 \equiv \delta$, $\gamma_1 \equiv \delta$, $\gamma_2 \equiv \tau^3\delta$, and $\alpha=\tau^{-6}$ [after Eq. (5)], where $\tau=(1+\sqrt{5})/2$ is the golden mean.[28,29] Plugging these values in Eq. (14), we get $\eta=(1+\tau^6)\delta^2 \simeq 0.2728\ldots$ eV^{-2}. By comparing this figure with those previously obtained for the samples discussed in Fig. 2, we realize that the role of electronic structure effects is quite remarkable in the ideal self-similar case. In Fig. 3, we show the corresponding $L(T)/L_0$ curve obtained from Eq. (8). As we can see, the presence of self-similar features in the electronic model parameters gives rise to an appreciable enhancement of the Lorenz function as the temperature is progressively increased.

IV. CONCLUSIONS

By comparing the overall $L(T)$ curves corresponding to the ideal case $q_1=0$ and those obtained for real samples with relatively small q_1 values in Fig. 2, we realize that the main qualitative features of the Lorenz curve do not sensitively depend on the precise value of the adopted q_1 value (provided it is small enough). Accordingly, we can confidently

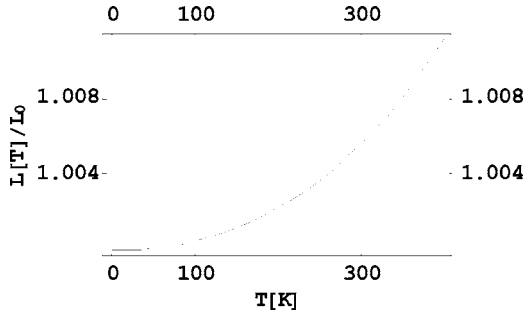

FIG. 3. Temperature variation of the normalized Lorenz function for an ideal QC characterized by a self-similar electronic structure model given by $\delta_1 \equiv -\tau^3\delta$, $\delta_2 \equiv \delta$, $\gamma_1 \equiv \delta$, $\gamma_2 \equiv \tau^3\delta$, and $\alpha=\tau^{-6}$, with $\delta=0.12$ eV.

conclude that the WFL anomaly is a generic feature of realistic QCs, presumably related to certain self-similar features in their electronic structure, as illustrated in Fig. 3. On the basis of this study, we propose the use of the expression $\kappa_{ph}=\kappa_{mes}-L(T)T\sigma$, where the Lorenz function is given by Eq. (8), instead of the usual assumption $L(T)\simeq L_0$, in order to properly determine the phonon contribution to the thermal conductivity in AlCu(Fe,Ru) and AlPd(Mn,Re) QCs and approximant phases.

ACKNOWLEDGMENTS

We warmly thank Tsunehiro Takeuchi for enlightening comments. We acknowledge M. V. Hernández for a critical reading of the paper. This work has been supported by the Universidad Complutense de Madrid through Project No. PR27/05-14014-BSCH.

APPENDIX

Taking into account the Fourier transform relationship

$$\frac{1}{x^2+a^2}=\frac{1}{2a}\int_{-\infty}^{\infty}e^{-a\omega}e^{i\omega x}\,d\omega,$$

the auxiliary integral H_0 can be properly rearranged in the form

$$H_0(\beta)\equiv\frac{\beta^2}{2a}\int_{-\infty}^{\infty}e^{-a\omega}\,d\omega\int_{-\infty}^{\infty}e^{i\omega x}\,\mathrm{sech}^2\left(\frac{x}{2}\right)dx, \quad \text{(A1)}$$

where $a^2\equiv q_0\beta^2$. Now, the second integral in Eq. (A1) is just the Fourier transform of the function $4\pi\omega\,\mathrm{cosech}(\pi\omega)$, so that we finally obtain

$$H_0\equiv\frac{2\pi\beta^2}{a}\int_{-\infty}^{\infty}e^{-a\omega}\omega\,\mathrm{cosech}(\pi\omega)d\omega=h_0\beta\zeta_H\left(2,\frac{1}{2}+\frac{\beta}{\pi^2h_0}\right),$$

with $h_0\equiv 2/(\pi\sqrt{q_0})$.

*Electronic address: emaciaba@fis.ucm.es

[1] G. D. Mahan and M. Bartkowiak, Appl. Phys. Lett. **74**, 953 (1999).
[2] J. M. Ziman, *Electrons and Phonons* (Clarendon, Oxford, 1960), p. 270.
[3] N. W. Ashcroft and N. D. Mermin, *Solid State Physics* (Saunders College Publishing, Cornell, 1976), p. 255.
[4] Yu. K. Vekilov, E. I. Isaev, and B. Johansson, Phys. Lett. A **352**, 524 (2006).
[5] B. D. Biggs, S. J. Poon, and N. R. Munirathmam, Phys. Rev. Lett. **65**, 2700 (1990).
[6] T. Klein, C. Berger, D. Mayou, and F. Cyrot-Lackmann, Phys. Rev. Lett. **66**, 2907 (1991).
[7] A. Carlsson, Nature (London) **353**, 353 (1991).
[8] R. Tamura, A. Waseda, K. Kimura, and H. Ino, Phys. Rev. B **50**, 9640 (1994).
[9] E. Maciá, Rep. Prog. Phys. **69**, 397 (2006).
[10] D. Mayou, in *Quasicrystals Current Topics*, edited by E. Belin-Ferré, C. Berger, M. Quiquandon, and A. Sadoc (World Scientific, London, 2000), p. 445.
[11] H. Solbrig and C. V. Landauro, Physica B **292**, 47 (2000).
[12] C. V. Landauro and H. Solbrig, Mater. Sci. Eng., A **294–296**, 600 (2000).
[13] C. V. Landauro and H. Solbrig, Physica B **301**, 267 (2001).
[14] H. Solbrig and C. V. Landauro, Adv. Solid State Phys. **42**, 151 (2002).
[15] E. Maciá, J. Appl. Phys. **93**, 1014 (2003).
[16] E. Maciá, Phys. Rev. B **69**, 132201 (2004).
[17] E. Maciá, T. Takeuchi, and T. Otagiri, Phys. Rev. B **72**, 174208 (2005).
[18] E. Maciá, Appl. Phys. Lett. **81**, 88 (2002).
[19] C. V. Landauro, E. Maciá, and H. Solbrig, Phys. Rev. B **67**, 184206 (2003).
[20] E. Maciá, Phys. Rev. B **69**, 184202 (2004).
[21] T. M. Apostol, *Introduction to Analytic Number Theory* (Springer-Verlag, New York, 1995).
[22] In agreement with the numerical results discussed in Ref. 19. Conversely, in Ref. 18 $\lim_{T\to 0}L(T)\simeq 0.9L_0$ was obtained due to truncation effects in the Taylor series expansion of the spectral conductivity function.
[23] J. M. Dubois, *Useful Quasicrystals* (World Scientific, New Jersey, 2005), p. 138.
[24] A. Perrot and J. M. Dubois, Ann. Chim. (Paris) **18**, 501 (1993).
[25] Z. Bihar, A. Bilusic, J. Lukatela, A. Smontara, P. Leglic, P. J. McGuiness, J. Dolinsek, A. Jaglicic, J. Jamovec, V. Demange, and J. M. Dubois, J. Alloys Compd. **407**, 65 (2006).
[26] K. Giannó, A. V. Sologubenko, M. A. Chernikov, H. R. Ott, I. R. Fisher, and P. C. Canfield, Phys. Rev. B **62**, 292 (2000).
[27] T. Takeuchi, N. Nagasako, R. Asahi, and U. Mizutani, Phys. Rev. B **74**, 054206 (2006).
[28] C. Janot and M. de Boissieu, Phys. Rev. Lett. **72**, 1674 (1994); C. Janot, Phys. Rev. B **53**, 181 (1996).
[29] E. Maciá, Phys. Rev. B **61**, 8771 (2000).